submitted to : ApJ

Black hole masses and Doppler factors of γ-ray active galactic nuclei

Zhong-Hui Fan[1], and Xinwu Cao[2]

Shanghai Astronomical Observatory, Chinese Academy of Sciences, Shanghai, 200030, China

ABSTRACT

The sizes of the broad-line regions (BLRs) in γ-ray active galactic nuclei (AGNs) are estimated from their optical continuum luminosity by using the empirical relation between $R_{\rm BLR}$ and $L_{\lambda,\rm opt}$. Using the broad emission line data, we derive the photon energy density in the relativistic blobs near the massive black holes in AGNs. We calculate the power of the broad-line photons Compton up-scattered by the relativistic electrons in the blobs. Compared with observed γ-ray emission data, the Doppler factors δ of the blobs for a sample of 36 γ-ray AGNs are derived, which are in the range of $\sim 3-17$. We estimate the central black hole masses of these γ-ray AGNs from the sizes of the BLR and the broad line widths. It is found that the black hole masses are in the range of $\sim 10^8-10^{10}M_\odot$. A significant correlation is found between the Doppler factor δ and the core dominance parameter R. The results are consistent with the external radiation Compton (ERC) models for γ-ray emission from AGNs. The soft seed photons are probably from the broad-line regions.

Subject headings: galaxies: active — gamma rays: theory — radiation mechanisms: nonthermal — black hole physics

[1]Email: fanzh@center.shao.ac.cn

[2]Email: cxw@center.shao.ac.cn

1. Introduction

All γ-ray AGNs are identified as flat-spectrum radio sources. The third catalog of high-energy γ-ray sources detected by the Energetic Gamma Ray Experiment Telescope (EGRET) on the Compton Gamma Ray Observatory (CGRO) includes 66 high-confidence identifications of blazars and 27 lower confidence potential blazar identifications (Hartman et al. 1999). This offers a good sample for the explorations on the radiative mechanisms of γ-rays from AGNs. The violent variations in very short time-scales imply that the γ-ray emission is closely related with the relativistic jets in blazars. There are two kinds of models, namely, leptonic models and hadronic models, proposed for γ-ray emission in blazars (see Mukherjee 2001 for a review). According to the different origins of the soft photons, the leptonic models can be classified as two groups: synchrotron self-Compton (SSC) models and ERC models (see Sikora & Madejski 2001 for a review).

In the frame of SSC models, the synchrotron photons are both produced and Compton up-scattered by the same population of relativistic electrons in the jets of γ-ray blazars. The synchrotron radiation is responsible for the low energy component in radio bands, and the synchrotron photons are Compton up-scattered to γ-ray photons by the same population of relativistic electrons in the jets (Maraschi, Ghisellini & Celotti 1992). However, SSC models meet difficulties with the observed rapidly variable fluxes in MeV-GeV for some blazars. It has been realized that the processes other than SSC may occur at least in some γ-ray blazars. One possibility is soft seed photons being from the external radiation fields outside the jets, namely, ERC models. The origins of soft seed photons may include the cosmic microwave background radiation, the radiation of the accretion disk (including photons from the disk scattered by surrounding gas and dust), infrared emission from the dust or/and a putative molecular torus, and broad-line regions, etc (Dermer & Schlickeiser 2002). Recently, Sikora et al. (2002) proposed that the external radiation is from the BLRs for GeV γ-ray blazars with flat γ-ray spectra, while the near-IR radiation from the hot dust is responsible for MeV γ-ray blazars with steep γ-ray spectra. In their model, the electrons are assumed to be accelerated via a two-step process and their injection function takes the form of a double power law with a break at the energy that divides the regimes for two different electron acceleration mechanisms.

The Doppler boosting factor δ of the jets is a crucial quantity in studying the physical processes at work in the regions near the massive black holes in AGNs. Several different approaches are proposed to estimate the Doppler factors δ of the jets in AGNs. Ghistellini et al. (1993) derived the synchrotron self-Compton Doppler factor $\delta_{\rm SSC}$ of the jets in AGNs from the VLBI core sizes and fluxes, and X-ray fluxes, on the assumption of the X-ray emission being produced by the SSC processes in the jets. Güijosa & Daly (1996) assumed

energy equipartition between the particles and the magnetic fields in the jet components, and derived the equipartition Doppler factor $\delta_{\rm eq}$. More recently, the variability Doppler factor $\delta_{\rm var}$ is derived on the assumption that the associated variability brightness temperature of total radio flux density flares are caused by the relativistic jets (Lähteenmäki & Valtaoja 1999).

In this paper, we use broad-line and γ-ray emission data to derive the Doppler boosting factors δ_γ for a sample of γ-ray blazars in the frame of the ERC model. The cosmological parameters H_0=75 km s^{-1}Mpc^{-1} and q_0=0.5 have been adopted in this work.

2. Model

2.1. Inverse Compton radiative processes

In this work, we calculate the power of γ-ray emission from blazars by the external Compton processes mainly following the calculations of Dermer, Sturner & Schlickeiser (1997). We then extend it to the case of the soft seed photons being from the BLRs of the blazars.

Assuming that blobs are moving with a constant velocity at an angle $\mu_{\rm obs}$=cos i with respect to the line of sight, we have the inverse Compton scattered γ-ray flux density $S_{\rm C}$ (Dermer, Sturner & Schlickeiser 1997):

$$S_{\rm C}=\frac{\delta_\gamma^{4+2\alpha}}{\alpha+2}\frac{c\sigma_{\rm T}u_{\rm i}^{*}n_{\rm eo}V_{\rm b}}{16\pi d_{\rm L}^2}(1+z)^{1-\alpha}\frac{(1+\mu_{\rm obs})^{2+\alpha}}{\mu_{\rm obs}}\frac{\epsilon_{\rm obs}^{-\alpha}}{(\overline{\epsilon}^{*})^{1-\alpha}}, \quad (1)$$

where δ_γ is the Doppler factor, α is the γ-ray photon energy spectral index, z is the cosmological redshift, $u_{\rm i}^{*}$ is the energy density of the soft seed photons in the blob's frame in units of ergs cm^{-3}, $d_{\rm L}$ is the luminosity distance, $\overline{\epsilon}^{*}$ is the dimensionless monochromatic mean soft photon energy in units of the electron rest mass energy, $n_{\rm eo}$ is the number density of electron in the blob, $V_{\rm b}$ is the volume of the blob, and $\sigma_{\rm T}$ is the Thomson cross section.

An optically thin, homogenous spherical blob is assumed to be located very near the central black hole, so most of the soft seed photons from the BLRs only experience one or a few inverse Compton scatters in the blob. The total cross section $S_{\rm T}\simeq\sigma_{\rm T}n_{\rm eo}V_{\rm b}=\xi\pi r_{\rm b}^2$, where $r_{\rm b}$ is the radius of the blob. For the homogenous spherical blob, we have $\xi=4\tau/3$, where $\tau=\sigma_{\rm T}n_{\rm eo}r_{\rm b}$ is the optical depth of the blob. As we do not know the value of the electron density $n_{\rm eo}$ in the blob, the parameter ξ, which is required $\xi\leq 1$, is adopted to describe the optical depth of the blob in our calculations.

For γ-ray blazars, the jets are believed to move in the direction very close to the line of

sight, so $\mu_{\rm obs} \simeq 1$ is taken and Eq. (1) becomes

$$S_{\rm C} = \frac{\delta_\gamma^{4+2\alpha}}{\alpha+2}\frac{c\xi r_{\rm b}^2 u_{\rm i}^*}{16\pi d_{\rm L}^2}(1+z)^{1-\alpha}2^{2+\alpha}\frac{\epsilon_{\rm obs}^{-\alpha}}{(\overline{\epsilon}^*)^{1-\alpha}}. \quad (2)$$

The soft seed photons are assumed to be from the different line emission. The observed γ-ray flux density is the sum of inverse Compton scattered flux densities contributed by different emission lines:

$$S_{\rm C} = S_{\rm C,H\beta} + S_{\rm C,MgII} + S_{\rm C,CIV} + S_{\rm C,Ly\alpha}\cdots = \sum_{\rm i}^{\rm n} S_{\rm C,i}. \quad (3)$$

2.2. Size of the blob

The size of the blob can be estimated from the observed γ-ray variability time-scale. Hartman et al. (1996) derived the size of the blobs $\sim 100R_{\rm g}$ ($R_{\rm g} = 2GM_{\rm bh}/c^2$) from the time-scale for substantial γ-ray variations of 3C279, if a $10^8 M_\odot$ black hole is present in 3C279. Ghisellini & Madau (1996) derived the upper limit on the blob-to-disc distance from the observed variability timescale $t_{\rm var}$ of the γ-ray fluxes. As the timescale $t_{\rm var} \sim (r_{\rm b}/\delta c)$, the radii of the blobs are around $3\times10^{16}(t_{\rm var}/d)(\delta/10)$ cm. As the typical variable timescale, $t_{\rm var} \sim 1$ day, we can infer the radii of the blobs are $\sim 3\times10^{16}$ cm if the Doppler factor $\delta \sim 10$ is adopted. For typical radio-loud quasars having masses of black holes around $10^9 M_\odot$, so the radii $r_{\rm b}$ of the blobs are around $200R_{\rm g}$. Montigny et al. (1997) employed the ERC model to explain γ-ray emission from the blazars. The comparisons of their model with the observed spectrum of 3C273 give the radius of the blob $r_{\rm b} \sim 2\times10^{16}$ cm. The central black hole mass of 3C273 is around $5.5\times10^8 M_\odot$ (Kaspi et al. 2000). Thus, we get $r_{\rm b} \sim 123R_{\rm g}$ for the blob in 3C273. In this paper, we take $r_{\rm b} = 120R_{\rm g}$ in our calculations.

2.3. Soft photon energy density in the blob's flame

The observed flux of the broad emission line is

$$f_{\rm line,i} = \frac{L_{\rm BLR,i}}{4\pi d_{\rm L}^2}, \quad (4)$$

where $L_{\rm BLR,i}$ is the luminosity of a single broad emission line.

The energy density of this emission line in the blob is given by

$$u_{\rm i}^* = \frac{1}{c}\left(\frac{d_{\rm L}}{R_{\rm BLR,i}}\right)^2 f_{\rm line,i}, \quad (5)$$

where $u_{\rm i}^{*}$ is monochromatic seed photon energy density of the broad line in the blobs and $R_{\rm BLR,i}$ is the radius of the BLR. The total soft seed photon energy density $u_{\rm tot}^{*} = \sum u_{\rm i}^{*}$ is the sum of all emission lines. Eq. (5) is only valid for the blob near the central black hole. At further distance away from the central black hole, the energy density of BLR photons in the blob is anisotropic and can be treated analogously to the approach for the dust torus (Arbeiter, Pohl & Schlickeiser 2002). In this paper, however, we only consider the case of the blob being located near the central black hole.

2.4. Sizes of broad emission line regions

Based on the long-time observations of 17 nearby Seyfert 1 galaxies and 17 Palomar-Green quasars, Kaspi et al. (2000) found an empirical relation between the size of the BLR $R_{\rm BLR}$ of Hβ and the monochromatic continuum luminosity at 5100 Å:

$$R_{\rm BLR} = 32.9 \times \left(\frac{\lambda L_{5100}}{10^{37}{\rm W}}\right)^{0.7} {\rm lt-day}. \tag{6}$$

Mclure & Jarvis (2002) suggested that Mg II is a low-ionization line as Hβ, so that Mg II is expected to be produced in the same region as Hβ. For a sample of 22 objects, they found a correlation between the FWHM of Mg II and Hβ: $V_{\rm FWHM,MgII} \sim V_{\rm FWHM,H\beta}^{1.02}$. It is therefore reasonable to expect that Mg II and Hβ are produced in the same region. Using the same sample and the size of the BLR derived by Kaspi et al. (2000), they obtained a correlation between $R_{\rm BLR}$ and the monochromatic continuum luminosity at 3000 Å:

$$R_{\rm BLR} = 28.4 \times \left(\frac{\lambda L_{3000}}{10^{37}{\rm W}}\right)^{0.47} {\rm lt-day}, \tag{7}$$

which has been corrected to the cosmological parameters used in this paper.

Vestergaard (2002) suggested a relation between the black hole mass $M_{\rm bh,UV}$ and the monochromatic continuum luminosity at 1350 Å. The black hole mass $M_{\rm bh,UV}$ is the central black hole mass based on the calibration of the single-epoch UV spectral measurements. They derived

$$M_{\rm bh,UV} = 1.6 \times 10^{6} \left(\frac{V_{\rm FWHM,CIV}}{10^{3}{\rm kms^{-1}}}\right)^{2} \left(\frac{\lambda L_{1350}}{10^{37}{\rm W}}\right)^{0.7} M_{\odot}, \tag{8}$$

where $V_{\rm FWHM}$ is the full width at half-maximum of the line C IV. The relation between $R_{\rm BLR}$ and the monochromatic continuum luminosity at 1350 Å is therefore available:

$$R_{\rm BLR} = 10.9 \times \left(\frac{\lambda L_{1350}}{10^{37}{\rm W}}\right)^{0.7} {\rm lt-day}. \tag{9}$$

Now, we can derive the sizes of broad emission lines Hβ, Mg II, and C IV from the optical or UV continuum luminosity by using the empirical relations (6), (7) and (9), respectively.

2.5. The black hole mass

We can estimate the central black hole masses of AGNs on the assumption that the motions of the gases in BLRs are virilized from the width of the emission line, if the size of the BLR is available. We use the empirical relation between the size of the BLR $R_{\rm BLR}$ and the optical continuum luminosity L_λ given in last subsection to estimate the size of the BLR $R_{\rm BLR}$. The black hole mass is given by

$$M_{\rm bh} = 2.25 \times R_{\rm BLR} V^2_{\rm FWHM} G^{-1}, \tag{10}$$

if the FWHM of any broad-line of Hβ, Mg II, and C IV is available (Gu, Cao & Jiang 2001).

2.6. The Doppler factor δ_γ

The Doppler factor δ_γ is given by

$$\delta_\gamma = 2^{\frac{2-\alpha}{4+2\alpha}} (1+z)^{\frac{\alpha-1}{4+2\alpha}} (\alpha+2)^{\frac{1}{4+2\alpha}} \left(\frac{c\xi r_{\rm b}^2}{S_{\rm C} d_{\rm L}^2}\right)^{-\frac{1}{4+2\alpha}} \left(\sum \frac{u_{\rm i}^*}{(\overline{\epsilon}_{\rm i}^*)^{1-\alpha}}\right)^{-\frac{1}{4+2\alpha}} \epsilon_{\rm obs}^{\frac{\alpha}{4+2\alpha}}. \tag{11}$$

Using the observed γ-ray flux, the Doppler factor δ_γ is available from Eq. (11), if the soft seed photon energy density $u_{\rm i}^*$ in the blob, the radius of the blob $r_{\rm b}$, and ξ are available. As the parameter ξ is required to be less than unit, we can obtain the lower limit of δ_γ, if $\xi = 1$ is adopted.

3. The sample

We search the literature and collect all available data of broad emission lines of γ-ray AGNs in EGRET catalog III. The selection criterion is that the sources of which the FWHM of at least one of the following broad emission lines Hβ, Mg II and C IV and the fluxes are available. This leads to 36 sources, of which 30 sources are the high-confidence identification blazars and 6 sources are the lower confidence potential blazar identifications listed in Hartman et al. (1999). For the source 0954+658, only the FWHM and the flux of the broad line Hα are available. We estimate the BLR size of Hα using the empirical relation $R_{\rm BLR}({\rm H}\alpha) = 1.19 {\rm R}_{\rm BLR}({\rm H}\beta)$ proposed by Kaspi et al. (2000).

In principle, all broad emission line fluxes are needed to calculate the total soft seed photon energy in the blobs contributed by different broad emission lines. Usually, the fluxes of only one or several broad emission lines are available for most sources in our sample due to the restriction of redshift. In our calculations, we consider fluxes for the following lines: Hβ, Mg II, C IV, C III, Lyα and Hα, which contribute about 60 per cent of the total broad line emission. We use the line ratios presented by Francis et al. (1991), in which the relative strength of Lyα is taken as 100, to calculate the total broad line emissions. Celotti, Padovani & Ghisellini (1997) added the contribution from the flux of Hα $F_{\rm H\alpha}$, with a value of 77. This gives a total relative flux $< F_{\rm BLR} >= 536.04$ (narrow lines are not included). For the lines Hβ, Mg II and C IV, we use Eq. (6), (7) and (9) to estimate their radii of the BLRs. For other lines of which the FWHM is available, we compare their FWHM with that of any one of those three lines Hβ, Mg II and C IV to estimate the radii of the BLRs. We use Eq. (5) to calculate the soft photon energy density in the blob for the lines with available FWHM and flux data. We calculate the total soft seed photon energy density $u^*_{\rm tot}$ in the blob as

$$u^*_{\rm tot} = \sum u^*_{\rm i} = 536.04 \times \frac{\sum_{\rm i} u^*_{\rm i,obs}}{\sum_{\rm i} F_{\rm i,re}}, \tag{12}$$

where $\sum_{\rm i} u^*_{\rm i,obs}$ is the photon density in the blob contributed by the lines with available emission line data, $\sum_{\rm i} F_{\rm i,re}$ is the sum of relative fluxes of these lines.

4. Results

Using the method described in § 2, we derive the parameters for all the sources in our sample. All the observational data and the results are listed in Tables $1-3$. The γ-ray emission is violently variable. For each source, we derived two values of the Doppler factor δ_γ corresponding to the lowest and highest values of the observed γ-ray fluxes.

In Figs. 1 and 2, we compare the Doppler factors δ_γ for the lowest and highest γ-ray flux cases with $\delta_{\rm var}$ derived from the variability time-scale of radio emission, respectively (Lähteenmäki & Valtaoja 1999). It is found that the values of $\delta_{\rm var}$ are higher than that of δ_γ for most sources in our sample.

In Fig. 3, we plot the relation between the core dominance parameter R and the Doppler factor $\delta_{\gamma,\rm min}$ derived from the lowest γ-ray flux. The core dominance parameters R are taken from Cao & Jiang (2001), except those of the sources of 0454−234, 0521−365 and 1741−038 taken from Dondi & Ghisellini (1995). A correlation between R and $\delta_{\gamma,\rm min}$ is found at a significant level of 97.5 per cent (Spearman correlation coefficient ρ). The results are plotted in Fig. 4 for the Doppler factor $\delta_{\gamma,\rm max}$ derived from the highest γ-ray flux. The significant level of the correlation becomes 95.2 per cent.

The distribution of the central black hole mass $M_{\rm bh}$ in γ-ray blazars is plotted in Fig. 5. The black hole masses $M_{\rm bh}$ are in the range of $10^8 - 10^{10} M_\odot$ with an average of around $2 \times 10^9 M_\odot$.

We plot the relation of the black hole mass $M_{\rm bh}$ with the lowest and highest γ-ray luminosity L_γ in Figs. 6 and 7, respectively. The correlations between them are found at the significant levels of 97.8 and 96.6 per cent for the lowest and highest γ-ray emissions, respectively.

5. Discussion

In this work, we estimate the size of the BLR from the optical or UV continuum luminosity. The observed optical/UV continuum emission from γ-ray blazars is a mixture of the emission from the disks and jets. The optical/UV continuum emission may be strongly beamed to us, since the viewing angles of the relativistic jets in these blazars are small. The emission from the jets may dominate over that from the disks at least in some blazars. So, the BLR size derived from the observed optical/UV continuum luminosity may be over estimated, and the derived black hole mass is a upper limit (Gu, Cao & Jiang 2001).

The size of the blob $r_{\rm b}$ is assumed to be $120 R_{\rm g}$ in our calculations (see discussion in Section § 2.2). As the black hole mass $M_{\rm bh}$ is derived from the size of the BLR and the line width, the size of the blob $r_{\rm b}$ is proportional to the BLR size $R_{\rm BLR}$. From Eq. (5), we know that the energy density in the blob $u^* \propto 1/R_{\rm BLR}^2$. The derived Doppler factor δ_γ in this work is therefore independent of the BLR size $R_{\rm BLR}$ (see Eq. (11)). It indicates that the overestimate of the BLR size caused by the contamination of the optical/UV continuum emission has not affected the values of derived Doppler factor δ_γ.

In our calculations, we adopted a parameter ξ to describe the optical depth of the blob, since we do not know the exact value of the actual number density $n_{\rm eo}$ of the electrons in the blob. From Eq. (11), it is found that the Doppler factor $\delta_\gamma \propto \xi^{-1/(4+2\alpha)}$. For a typical value of $\alpha \sim 1.5$, we found that the derived δ_γ becomes about twice of its initial value, if the parameter ξ is changed from 1 to 0.01. The uncertainty of ξ in our calculations would not affect our results significantly.

We only consider the photons from the BLRs as the soft seed photons. Other sources of soft seed photons (e.g., emission from the disks, synchrocyclotron emission in the blobs, etc.) have not been included in the calculations. The Doppler factor δ_γ derived in this work are in the range of 3.04 and 17.00, if $\xi = 1$ is adopted. It is generally consistent with the results derived by other methods (Ghistellini et al. 1993; Güijosa & Daly 1996; Lähteenmäki &

Valtaoja 1999). It may imply that the soft seed photons are indeed mainly from the BLRs in these sources.

The variability Doppler factors $\delta_{\rm var}$ of 20 γ-ray blazars in our sample have been derived from the radio variable time-scales are available (Lähteenmäki & Valtaoja 1999). Comparing with the Doppler factors δ_γ derived in this work, we find that the variability Doppler factor $\delta_{\rm var}$ are higher than δ_γ derived in this work for most sources (see Figs. 1 and 2). This may be due to the fact that we adopt $\xi = 1$ and the derived Doppler factor δ_γ are then the lower limits. The value of ξ may possibly be estimated roughly by letting $\delta_{var} = \delta_\gamma$. It can be found that the values of ξ can be low as $10^{-3} - 10^{-2}$ for some sources (see Eq. (11), Figs. 1 and 2).

The core dominance parameter $R = f_{\rm c}/f_{\rm e}$, where $f_{\rm c}$ and $f_{\rm e}$ are the core and extended flux densities at 5 GHz in the rest frame of the source. The core dominance parameter R is believed to be a good indicator of the Doppler factor of the jet. We find a significant correlation between the core dominance parameter R and the derived Doppler factor δ_γ. This implies that the derived Doppler factors δ_γ are reliable for the γ-ray blazars in this sample and the soft seed photons are mainly from the BLRs.

It was argued that the SSC radiative mechanism is dominant in BL Lac objects (Sikora et al. 2002). However, we cannot find significant differences between BL Lac objects and quasars in our investigations. The reason may be that the BL Lac objects in our sample have relative stronger broad line emission compared with other BL Lac objects listed in EGRET catalog III, since we only select the γ-ray blazars with broad-line emission data as our sample. So these BL Lac objects in our sample are more like quasars as they have rather strong broad-line emission (Véron-Cetty & Véron 2000). For these BL Lac objects with relative strong broad-line emission, the ERC radiative mechanism may probably be important as that in quasars.

The black hole masses of γ-ray blazars in this sample are in the range of $10^8 - 10^{10} M_\odot$. This is consistent with some previous results for radio-loud AGNs (Mclure & Dunlop 2001; Laor 2000). We have found significant correlations between the black hole mass $M_{\rm bh}$ and the γ-ray luminosity L_γ. The reason may be that the γ-ray flux depends sensitively on the Doppler factor δ_γ and the values of the Doppler factor of the γ-ray AGNs in our sample spread over a large range ($\sim 3 - 17$). On the other hand, it is expected that the γ-ray flux is independent of the black hole mass in ERC mechanisms with the soft seed photons being from the BLRs (see Eq. (2) and discussion in the second paragraph of this section).

This work is supported by NSFC(No. 10173016) and the NKBRSF (No. G1999075403). This research has made use of the NASA/IPAC Extragalactic Database (NED), which is

operated by the Jet Propulsion Laboratory, California Institute of Technology, under contract with the National Aeronautic and Space Administration.

REFERENCES

Arbeiter, C., Pohl, M., & Schlickeiser, R. 2002, A&A, 386, 415

Baldwin, J. A. 1975, ApJ, 201, 26

Baldwin, J. A., Wampler, E. J., & Gaskell, C. M. 1989, ApJ, 338, 630

Cao, X., & Jiang, D. R. 2001, MNRAS, 320, 347

Celotti, A., Padovani, P., & Ghisellini, G. 1997, MNRAS, 286, 415

Corbin, M. R. 1992, ApJ, 391, 577

Corbin, M. R., & Boroson, T. A. 1996, ApJS, 107, 69

Dermer, C. D., Sturner, S. J., Schlickeiser, R. 1997, ApJS, 109, 103

Dermer, C. D., & Schlickeiser, R. 2002, ApJ, 575, 667

Dondi, L., & Ghisellini, G. 1995, MNRAS, 273, 583

Francis, P. J., Hewett, P. C., Foltz, C. B., Chaffee, F. H., Weymann, R. J., Morris, S. L. 1991, ApJ, 373, 465

Fricke, K. J., Kollatschny, W., & Witzel, A. 1983, A&A, 117, 60

Ghiselini, G., Padovani, P., Celotti, A., & Maraschi, L. 1993, ApJ, 407, 65

Ghisellini, G., & Madau, P. 1996, MNRAS, 280, 67

Gu, M. F, Cao, X., & Jiang, D. R. 2001, MNRAS, 327, 1111

Güijosa, A., & Daly, R. A. 1996, ApJ, 461, 600

Hartman, R. C., et al. 1996, ApJ, 461, 698

Hartman, R. C. et al. 1999, ApJS, 123, 79

Hunstead, R. W., Murdoch, H. S., & Shobbrook, R. R. 1978, MNRAS, 185, 149

Jackson, N., & Browne, W. A. 1991, MNRAS, 250, 414

Kaspi, S., Smith, P. S., Netzer, H., Maoz, D., Jannuzi, B. T., & Giveon, U. 2000, ApJ, 533, 631

Lähteenmäki, A., & Valtaoja, E. 1999, ApJ, 521, 493

Laro, A. 2000, ApJ, 543, 111

Lawrence, C. R., Zucker, J. R., Readhead, A. C. S., Unwin, S. C., Pearson, T. J., & Xu, W. 1996, ApJ, 107, 541

Maraschi, L., Ghisellini, G., & Celotti, A. 1992, ApJ, 397, L5

Mariziani, P., Sulentic, J. W., Dultzin-Hacyan, D., Calvani, M., & Moles, M. 1996, ApJS, 104, 37

Montigny, V. C., et al. 1997, ApJ, 483, 161

Mukherjee, R. 2001, in AIP Conf. Proc. 558, High Energy Gamma-Ray Astronomy, ed. by F. A. Aharonian & H. J. Völk (New York: AIP), 324

Mclure, R. J., & Dunlop, J. S. 2001, MNRAS, 327, 199

Mclure. R. J., & Jarvis., M. J. 2002, MNRAS, 337, 109

Osmer, P. S., Porter, A. C., Green, R. F. 1994, ApJ, 436, 678

Rudy, R. J. 1984, ApJ, 284, 33

Scarpa, R., & Falomo, R. 1997, A&A, 325, 109

Sikora, M., & Madejski, G. 2001, in AIP Conf. Proc. 558, High Energy Gamma-Ray Astronomy, ed. by F. A. Aharonian & H. J. Völk (New York: AIP), 275

Sikora, M., Blazejowki, M., Moderski, R., & Madejski, G. M. 2002, ApJ, 577, 78

Stickel, M., Fried, J. W., & Kühr, H. 1989, A&AS, 80, 103

Stickel, M., & Kühr, H. 1993, A&AS, 101, 521

Stickel, M., Kühr, H., & Fried, J. W. 1993,A&AS, 97, 483

Stockton, A., & Mackenty, J. W. 1987, ApJ, 316, 584

Ulrich, M. H., et al. 1980, MNRAS, 192, 561

Véron-Cetty, M. P., & Véron, P. 2000, A&A Rev., 10, 81

Vestergaard, M. 2002, ApJ, 571, 733

Wilkes, B. J. 1986, MNRAS, 218, 331

Wills, B. J., et al. 1995, ApJ, 447, 139

Table 1. Broad emission line data, black hole masses and γ-ray luminosities

Source	Redshift	Line	FWHM[a]	Ref.	log $M_{bh}/M_{\odot}$	log $L_{\gamma,min}$[b]	log $L_{\gamma,max}$[b]
0119+041[d]	0.637	Hβ	4444	G01	8.855[e]	46.309	46.909
0208−512[c]	1.003	Hβ	4070	W86	9.208	47.916	48.497
0336−019	0.852	Hβ	4875	G01	9.459[e]	47.903	48.580
0414−189	1.536	Mg II	1713	H78	8.075	47.310	47.996
0420−014	0.915	Hβ	3000	G01	9.510[e]	46.987	47.826
0440−003	0.844	Mg II	3900	B89	8.813	47.071	47.908
0454−234[c]	1.009	Mg II	7891	S89	9.173	46.823	47.082
0454−463	0.858	Mg II	2700	F83	8.626	46.587	47.204
0458−020	2.286	C IV	5200	B89	8.662	47.878	48.734
0521−365[c, d]	0.055	Hβ	6758	SK93	8.708	44.584	44.889
0537−441[c]	0.894	Mg II	3200	W86	8.709	47.228	47.970
0539−057[d]	0.839	Mg II	8598	S93	9.411	48.015	48.015
0804+499[d]	1.430	Mg II	2259	L96	8.634	47.522	47.781
0836+710	2.172	Mg II	3062	L96	9.450	47.723	48.312
0851+202[c]	0.306	Hβ	3441	S89	8.919	46.215	46.427
0954+556	0.901	C IV	10503	W95	9.718	46.990	47.851
0954+658[c]	0.368	Hα	2084	L96	8.526	46.182	46.618
1127−145[d]	1.187	Mg II	2750	W86	8.850	47.168	47.964
1222+216	0.435	Hβ	2197	SM87	8.435	46.235	47.078
1226+023	0.158	Hβ	3416	K00	9.298	45.268	46.026
1229−021	1.045	Mg II	5000	B89	9.118	46.698	47.199
1253−055[c]	0.538	Hβ	3100	G01	8.912[e]	46.770	48.229
1331+170	2.084	C IV	5740	C92	9.171	47.472	48.348
1334−127[c]	0.539	Mg II	7077	SK93	9.294	46.188	46.753
1424−418	1.522	Mg II	9144	S89	9.652	47.860	48.418
1504−166[d]	0.876	Mg II	5139	H78	9.130	47.450	47.754
1510−089	0.361	Hβ	3180	G01	9.130[e]	46.233	46.827
1611+343	1.401	Hβ	5600	G01	10.05[e]	47.716	48.276
1633+382	1.814	Mg II	9657	L96	10.09	48.332	48.861
1725+044	0.296	Hβ	2090	G01	8.545[e]	46.001	46.251
1739+522	1.375	Mg II	2559	L96	8.866	47.410	48.076
1741−038	1.054	Mg II	11574	S89	9.566	47.231	47.851
2230+114	1.037	C IV	3340	W95	9.164	47.217	47.847
2251+158	0.859	Hβ	2800	G01	9.644[e]	47.467	48.141
2320−035	1.411	C IV	3300	B89	8.079	47.605	48.273
2351+456	1.922	Mg II	5118	L96	9.190	47.867	48.427

[a]in unit of km s^{-1}

[b]in unit of ergs s^{-1}

[c]BL Lac object

[d]lower confidence potential blazar identifications

[e]the data of black hole masses from Gu, Cao & Jiang (2001)

References. — B89: Baldwin, Wampler & Gaskell (1989); C92: Corbin (1992); F83: Fricke, Kollatschny & Witzel (1983); G01: Gu, Cao & Jiang (2001); H78: Hunstead, Murdoch & Shobbrook (1978); K00: Kaspi et al. (2000); L96: Lawrence et al. (1996); S89: Stickel, Fried & Kühr (1989); S93: Stickel & Kühr (1993); SK93: Stickel, Kühr & Fried (1993); SM87: Stockton & Mackenty (1987); W86: Wilkes (1986); W95: Wills et al. (1995).

Table 2. Broad emission lines data and the total energy density of the blob

Source	Lines	References	log $u^*_{\rm tot}$
0119+041	Hβ	JB91	−1.896
0208−512	Mg II, C III	W86, S97	−2.461
0336−019	Hβ, Mg II, C III	B89, JB91	−2.794
0414−189	Mg II, C IV, C III	H78	+0.026
0420−014	Mg II, C III	B89, S97	−2.924
0440−003	Mg II	B89	−2.069
0454−234	Mg II, C III	S89	−1.872
0454−463	Mg II	F83	−1.837
0458−020	C IV	B89	−1.702
0521−365	Hβ	SK93	−2.722
0537−441	Mg II	W86, S97	−2.234
0539−057	Mg II	S93	−1.390
0804+449	Mg II, C IV, C III	L96	+0.411
0836+710	Mg II, C IV, C III, Lyα	L96	+0.258
0851+202	Hβ	S89	−4.109
0954+556	C IV, Lyα	W95	−2.063
0954+658	Hα	L96	−4.425
1127−145	Mg II, C IV, C III	W86, W95	−0.317
1222+216	Hβ	SM87	−2.109
1226+023	Hβ, Mg II, C IV, C III, Lyα, Hα	K00, U80, CB96, B87	−2.067
1229−021	Mg II	B98	−1.729
1253−055	Hβ, Mg II, C IV, C III, Lyα	W95, M96	−1.797
1331+170	C IV	C92	−1.716
1334−127	Mg II	SK93	−2.370
1424−418	Mg II, C III	S89	−2.194
1504−199	Mg II	H78	−1.898
1510−089	Hβ	O94	−2.595
1611+343	Hβ, C IV, C III, Lyα	W95	−3.075
1633+382	Mg II, C IV, C III, Lyα	L96	−2.537
1725+044	Hβ	R84	−2.819
1739+522	Mg II, C IV, C III	L96	−1.446
1741−038	Mg II	S89	−1.816
2230+114	C IV, C III, Lyα	W95	−1.856
2251+158	Hβ, C IV, C III, Lyα	W95	−2.632
2320−035	C IV	B89	−1.653
2351+456	Mg II, C IV, C III	L96	−1.480

References. — B75: Baldwin (1975); B89: Baldwin, Wampler & Gaskell (1989); C92: Corbin (1992); CB96: Corbin & Boroson (1996); F83: Fricke, Kollatschny & Witzel (1983); G01: Gu, Cao & Jiang (2001); H78: Hunstead, Murdoch & Shobbrook (1978); JB91: Jackson & Browne (1991); K00: Kaspi et al. (2000); L96: Lawrence et al. (1996); M96: Mariziani et al. (1996); O94: Osmer, Porter & Green (1994); R84: Rudy (1984); S97: Scarpa & Falomo (1997); S89: Stickel, Fried & Kühr (1989); S93: Stickel & Kühr (1993); SK93: Stickel, Kühr & Fried (1993); SM87: Stockton & Mackenty (1987); U80: Ulrich et al. (1980); W86: Wilkes (1986); W95: Wills et al. (1995).

Table 3. γ-ray fluxes, Doppler factors and core dominated parameters

Source	γ	$F_{\gamma,\min}$	$F_{\gamma,\max}$	$\delta_{\gamma,\min}$	$\delta_{\gamma,\max}$	$\delta_{\rm var}$	R
0119+041	2.63	5.1	20.3	5.98	7.23	...	15.85
0208−512	1.99	35.2	134.1	7.76	9.71	...	...
0336−019	1.84	37.4	177.6	7.27	9.56	19.01	31.62
0414−189	3.25	10.2	49.5	7.63	9.19	...	...
0420−014	2.44	9.3	64.2	6.61	8.75	11.72	251.3
0440−003	2.37	12.5	85.9	8.52	11.3	11.46	19.95
0454−234	3.14	8.1	14.7	5.94	6.39	...	5.00
0454−463	2.75	5.5	22.8	7.15	8.65	...	...
0458−020	2.45	9.5	68.2	10.1	13.5	17.80	5.01
0521−365	2.63	15.8	31.9	4.46	4.91	...	1.00
0537−441	2.41	16.5	91.1	9.03	11.6	...	199.6
0539−057	2.00	66.5	66.5	4.60	4.60	...	7.61
0804+499	2.15	8.3	15.1	3.82	4.20	26.21	151.9
0836+710	2.62	8.6	33.4	3.19	3.85	10.67	34.93
0851+202	2.03	9.7	15.8	9.62	10.4	18.03	781.0
0954+556	2.12	6.5	47.2	3.44	4.73	4.63	10.81
0954+658	2.08	6.6	18.0	14.5	17.0	6.62	110.5
1127−145	2.70	9.9	61.8	4.87	6.24	...	50.12
1222+216	2.28	6.9	48.1	7.12	9.57	8.16	...
1226+023	2.58	8.5	48.3	3.04	3.87	5.71	6.31
1229−021	2.85	4.9	15.5	5.45	6.33	...	3.43
1253−055	1.96	9.3	267.3	5.18	9.14	16.77	12.59
1331+170	2.41	4.4	33.1	6.20	8.34	...	...
1334−127	2.62	5.5	20.2	4.71	5.64	...	12.87
1424−418	2.13	15.3	55.3	5.28	6.48	...	2.38
1504−166	2.00	16.5	33.2	5.58	6.27	...	19.95
1510−089	2.47	12.6	49.4	5.84	7.11	13.18	31.62
1611+343	2.42	19.0	68.9	6.36	7.68	5.04	25.12
1633+382	2.15	31.8	107.5	5.22	6.33	8.83	79.44
1725+044	2.67	13.3	23.7	8.68	9.39	2.46	125.8
1739+522	2.42	9.7	44.9	6.72	8.40	12.12	50.1
1741−038	2.42	11.7	48.7	4.44	5.47	8.92	4.00
2230+114	2.45	12.1	51.6	5.92	7.31	14.23	25.12
2251+158	2.21	24.6	116.1	5.97	7.61	21.84	15.85
2320−035	2.00	8.2	38.2	12.1	15.6	...	...
2351+456	2.38	11.8	42.8	6.37	7.71	...	...

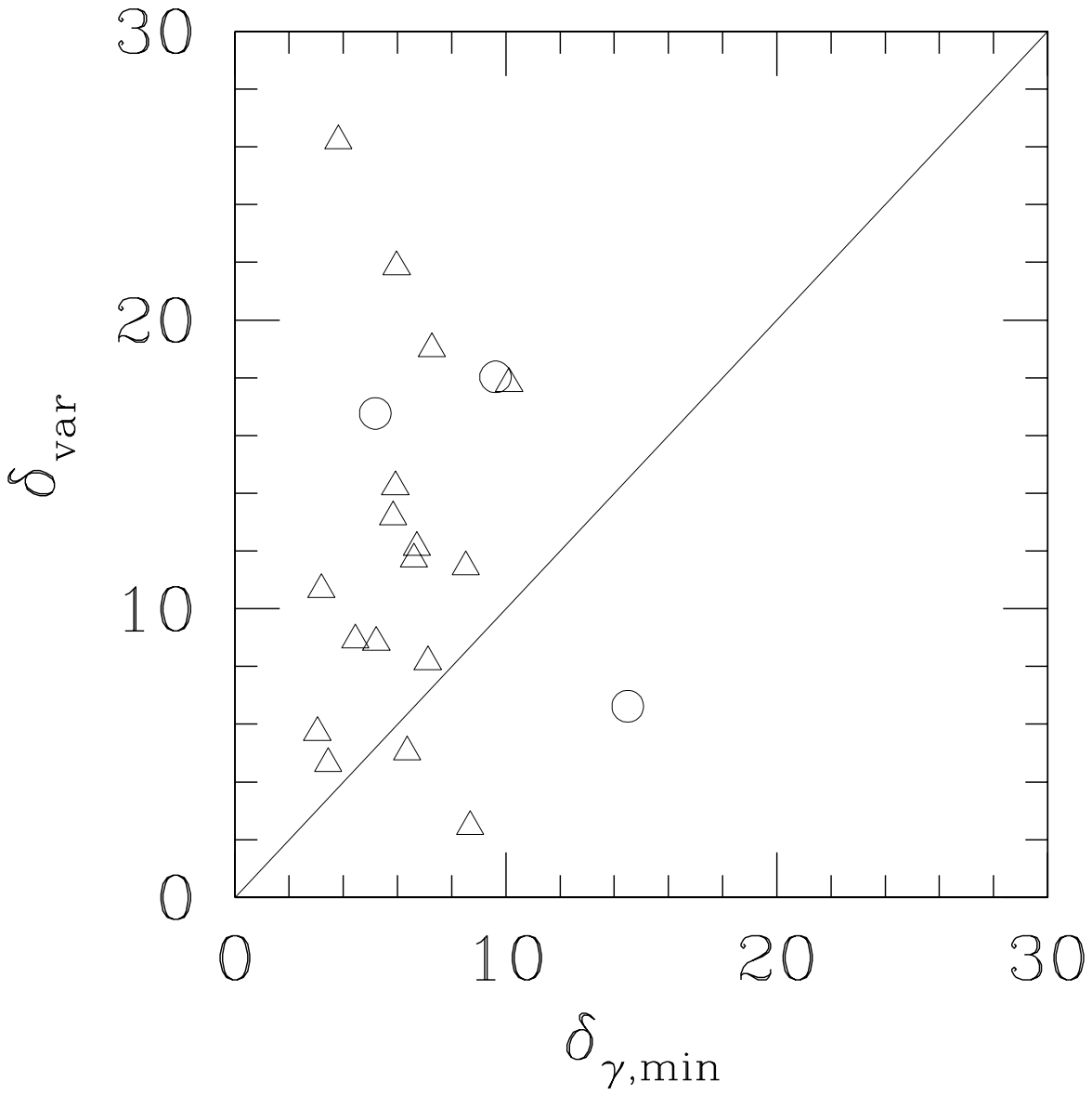

Fig. 1.— The variability Doppler factor $\delta_{\rm var}$ vs. the Doppler factor $\delta_{\gamma,\rm min}$ derived in this work. The circles represent BL Lac objects, while the triangles represent quasars.

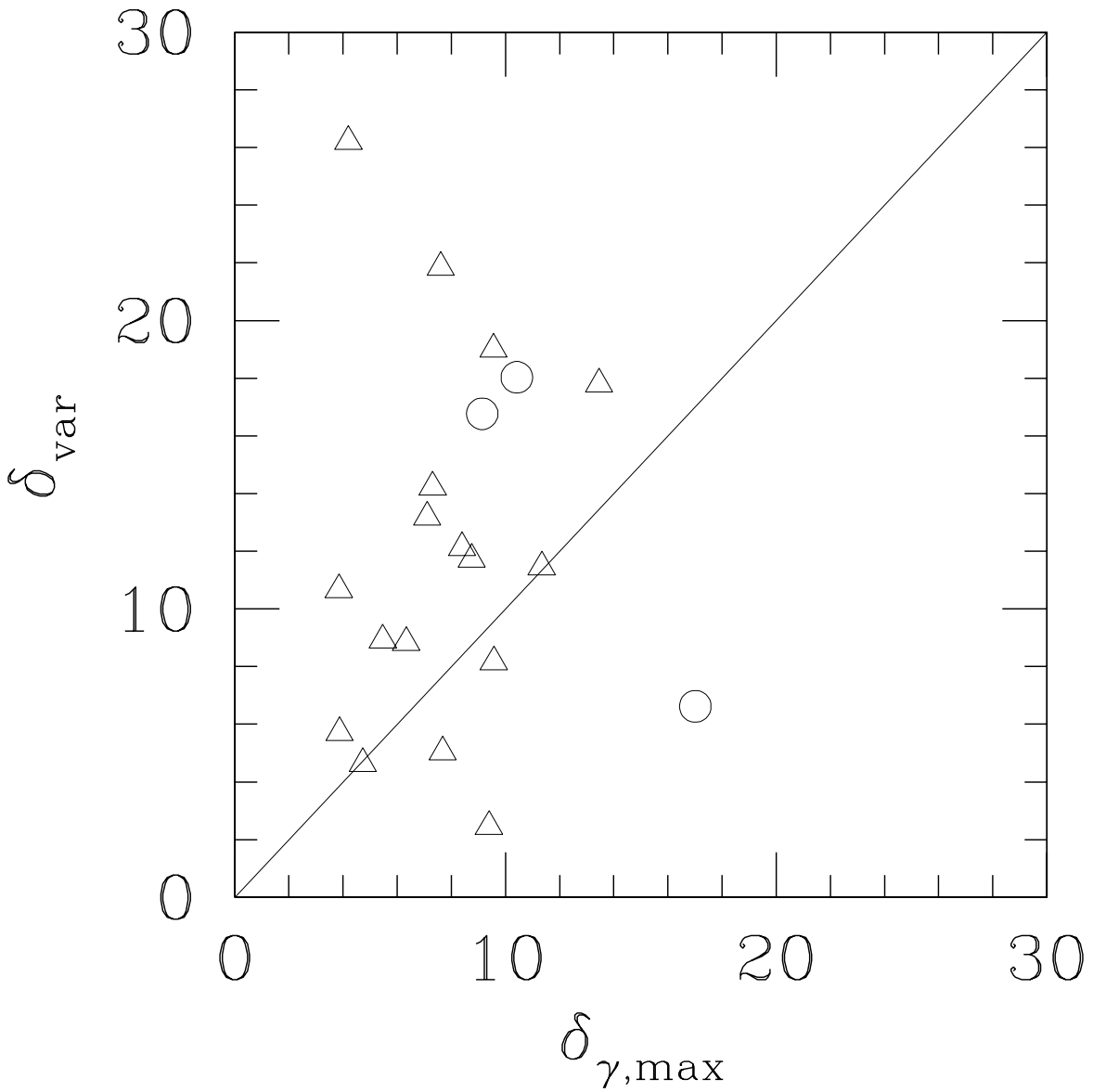

Fig. 2.— Same as Fig. 1, but the Doppler factor $\delta_{\gamma,\rm max}$ rederived from the highest γ-ray fluxes.

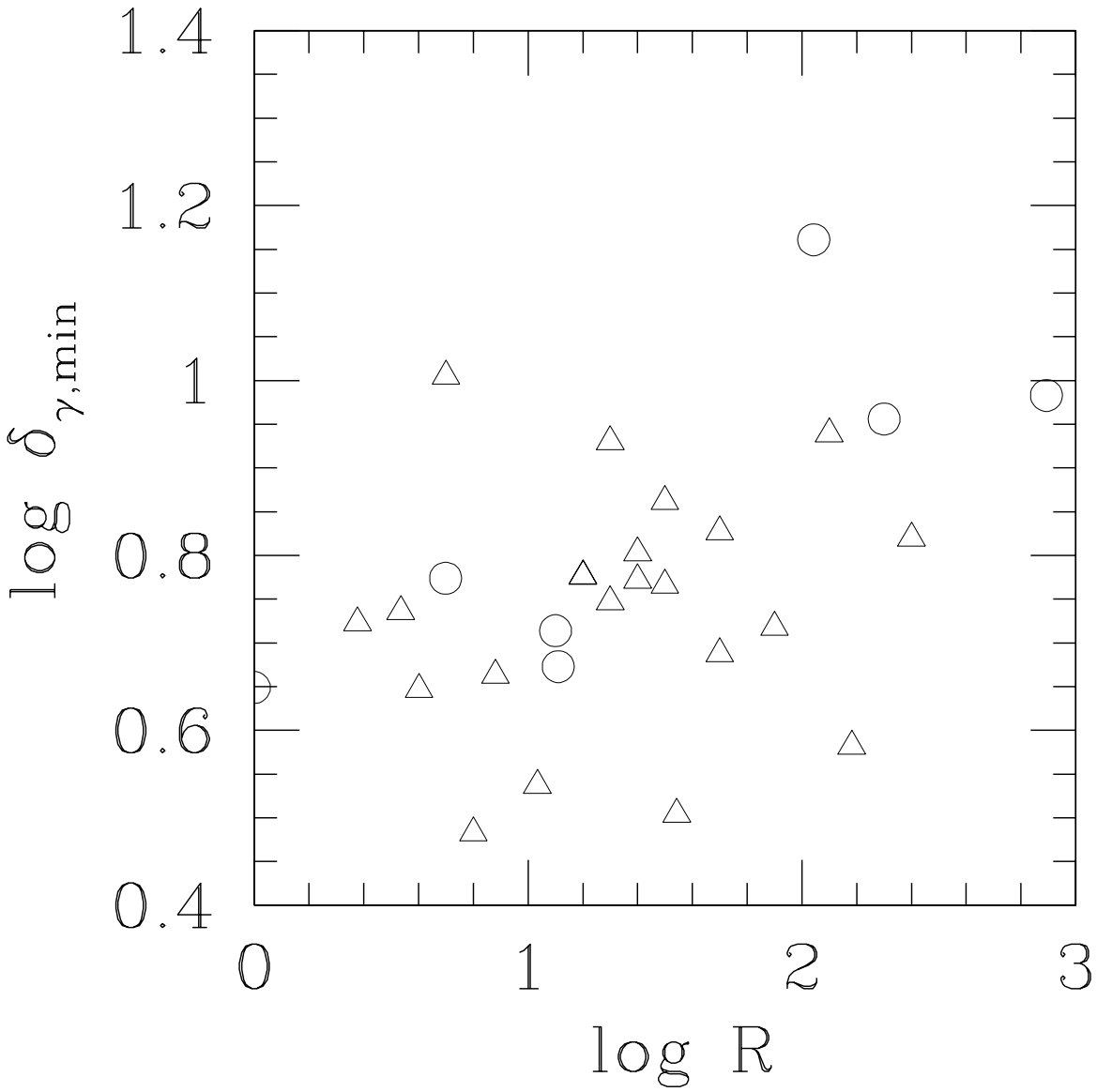

Fig. 3.— The core dominance parameter R vs. the Doppler factor $\delta_{\gamma,\mathrm{min}}$.

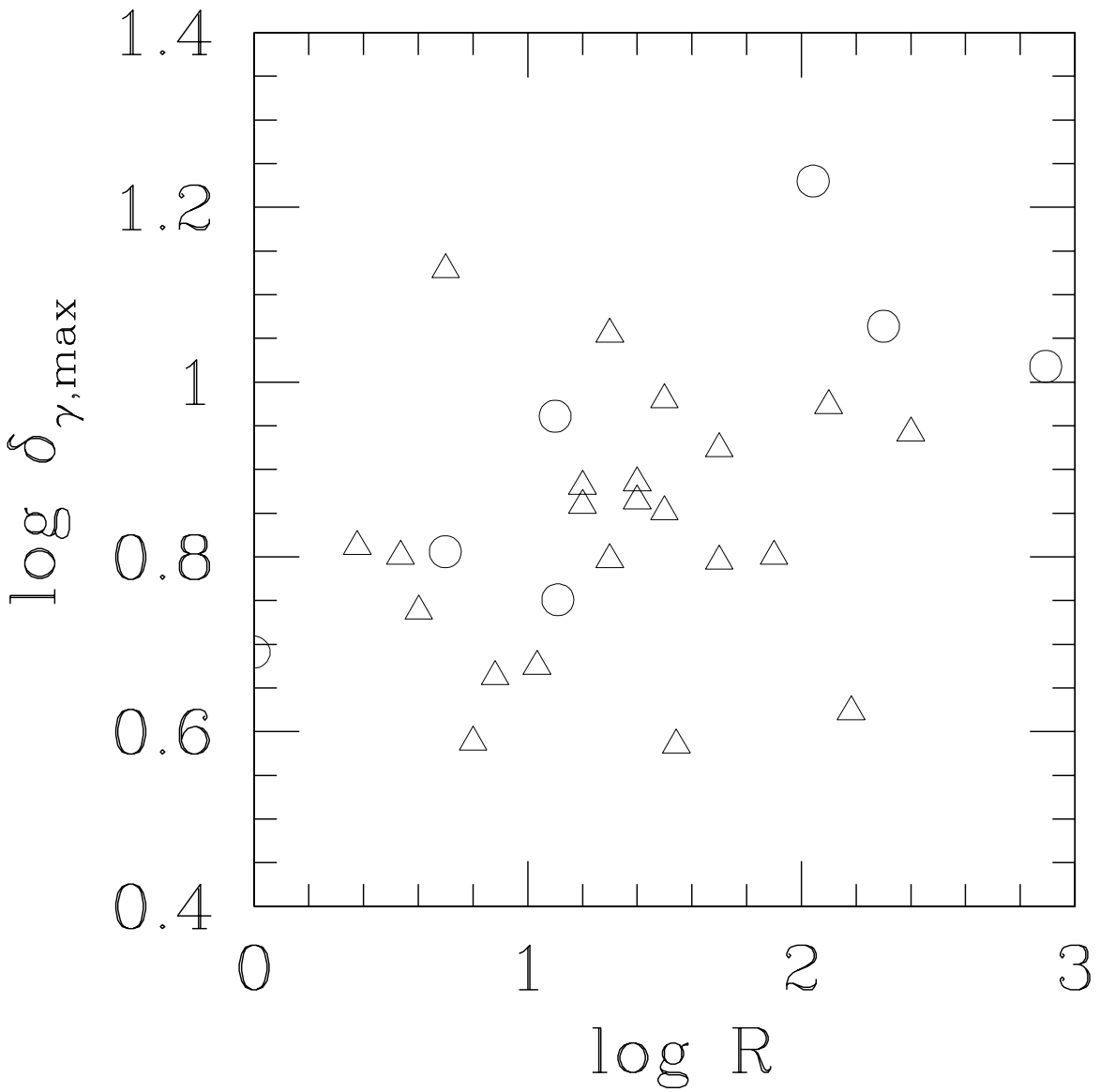

Fig. 4.— Same as Fig. 3, but the Doppler factor $\delta_{\gamma,\mathrm{max}}$ rederived from the highest γ-ray fluxes.

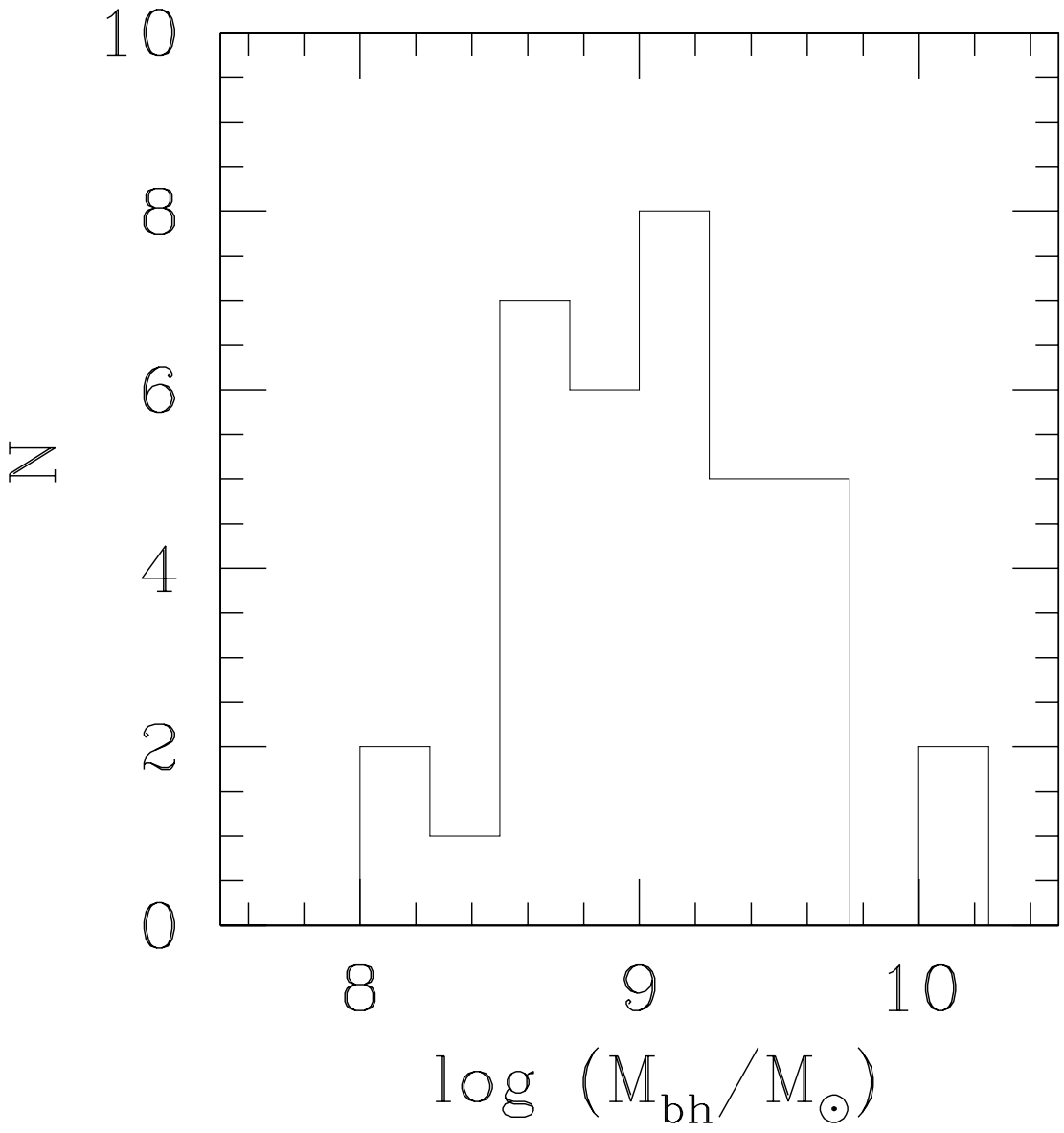

Fig. 5.— The distribution of the black hole masses.

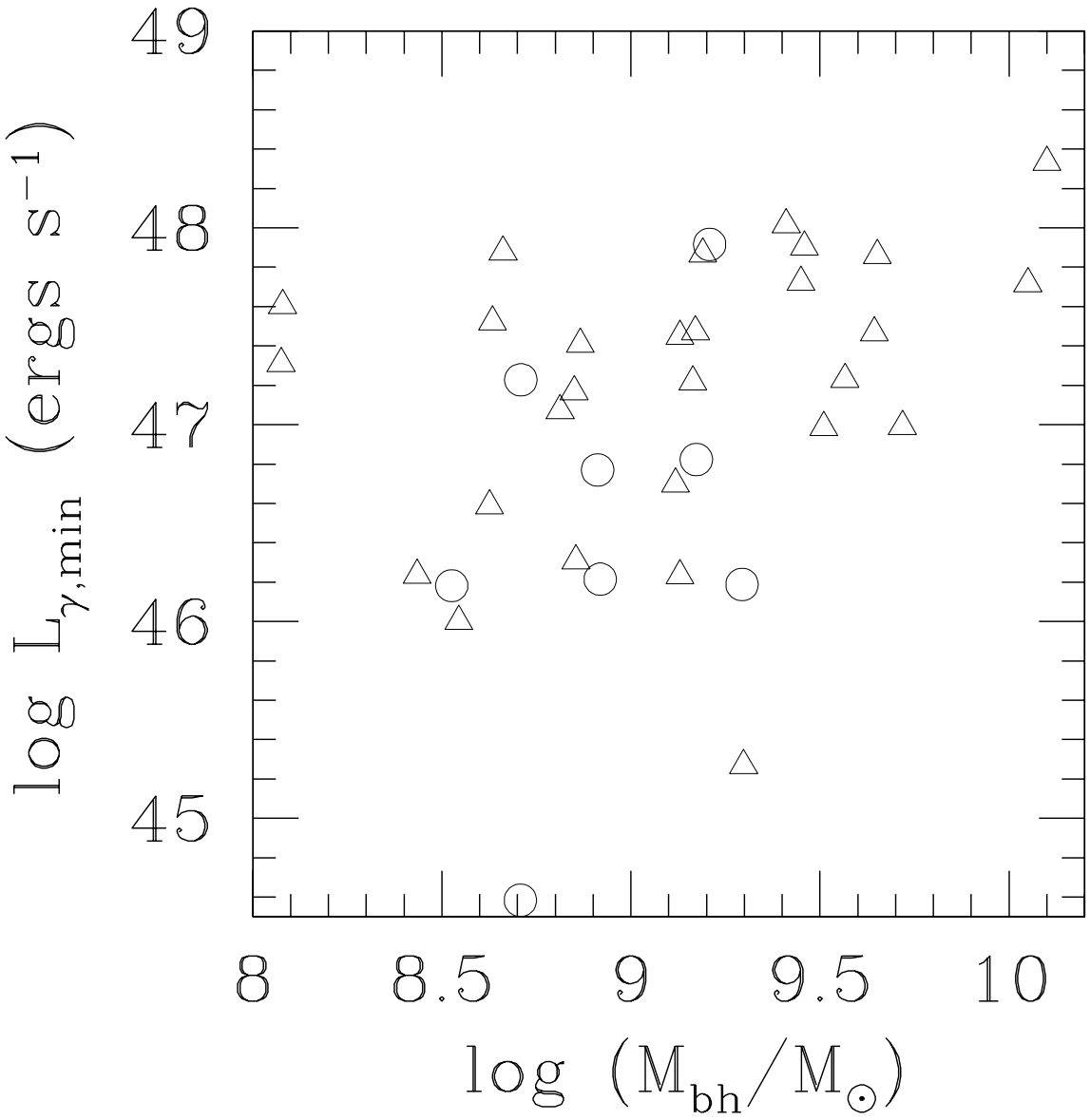

Fig. 6.— The lowest γ-ray luminosity $L_{\gamma,\mathrm{min}}$ vs. the black hole mass M_{bh}.

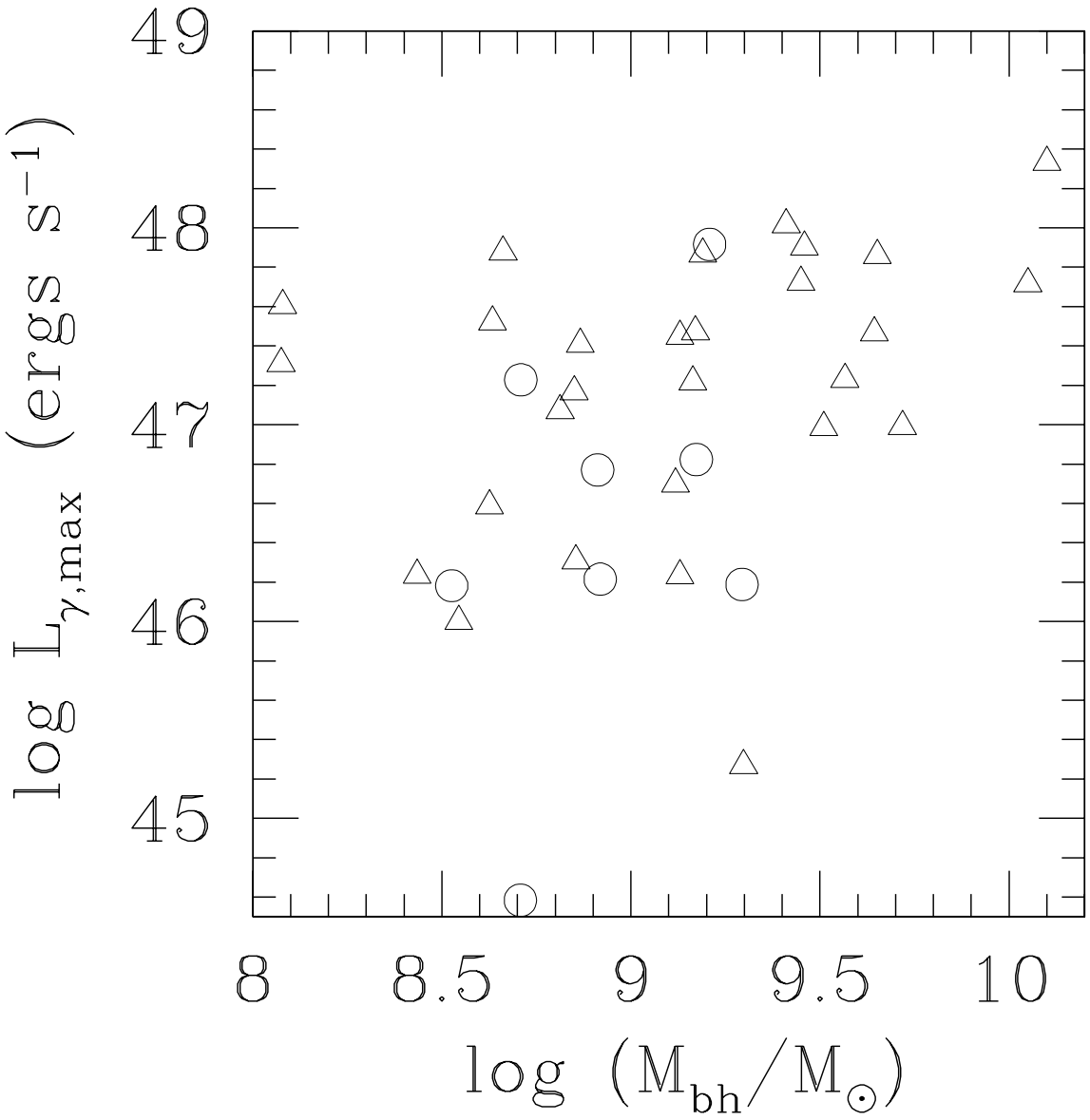

Fig. 7.— Same as Fig. 6, but for the highest γ-ray luminosity $L_{\gamma,max}$.